Theoretical Determination of Molecular Structure and Conformation. 16. Substituted Cyclopropanes—An Electron Density Model of Substituent-Ring Interactions

Dieter Cremer* and Elfi Kraka

Contribution from the Lehrstuhl für Theoretische Chemie, Universität Köln, D-5000 Köln 41, West Germany. Received October 10, 1984

Abstract: Investigation of the one-electron density distribution $\rho(r)$ and the associated Laplace distribution $\nabla^2\rho(r)$ for compounds CH_3X suggests a simple pattern of distortions of the valence sphere of C caused by the electronic influence of X. Electron attractors (repellers) pull (push) the valence sphere from (toward) the C nucleus, thus deshielding (shielding) it. In addition, distortions of the valence sphere reveal that geminal and vicinal charge concentrations possess a tendency of avoiding each other. On the basis of these observations an electron density model is developed in order to rationalize substituent (X) effects on ring strain and surface delocalization (σ-aromaticity) in substituted cyclopropanes **1** and to predict ring geometries for **1**. For test purposes 6-31G*//4-31G calculations are carried out for 12 different cyclopropanes (X = H, F, OH, NH_2, CH_3, CN, $CHCH_2$, CF_3, Li; X, Y = F, F; CH_3, CH_3; CF_3, CN) and eight 2-propanes (X = H, F, OH, NH_2, CH_3, CN, CF_3, Li). It is shown that electropositive substituents stabilize **1** due to a predominant enhancement of σ-aromaticity. The reverse is true for electronegative substituents like F or OH. In most other cases (X = CN, CF_3, etc.) changes in ring strain and σ-aromaticity cancel largely leaving the overall stability of cyclopropane essentially unchanged.

I. Introduction

The ability of cyclopropanes (**1**) to interact with π-electron acceptor substituents has been rationalized on the basis of the Walsh MO model of **1**.[1,2] Charge transfer from the antisymmetrical 3e' MO of **1** to a low-lying acceptor orbital of the substituent leads to a strengthening of the basal bond C_2C_3 and a weakening of the vicinal bonds C_1C_2 and C_1C_3 of **1**. This has been confirmed by experimentally and theoretically obtained structural data of substituted **1**.[3-6]

As for cyclopropanes with other than π-acceptor substituents, a variety of orbital interactions has been invoked to explain observed structural changes of the three-membered ring (3MR).[4-6] In general, it turned out difficult to make reliable predictions with regard to the dominating orbital interaction and the CC bond length changes resulting therefrom. In the case of π-donor substituents, in particular halogens like F and Cl, structural predictions based on the Walsh MOs of **1** were found to be at variance with experimental results.[5] A careful investigation of this conflict between theory and experiment showed that the usual techniques of MO theory, e.g., analysis of orbital correlation diagrams and overlap populations, lack their usual predictive power when applied

to fluoro-substituted cyclopropanes.[6] Consideration of electron density difference maps obtained by using **1** as a reference molecule turned out to be useful in some cases. At least it helped to resolve the conflict between theory and experiment in the case of halogen substitution of **1**.[6] However, no generally valid rules for substituent, ring interactions could be derived so far on the basis of either orbital or electron density studies. It seems that each substituted cyclopropane has to be considered separately.[4]

In this paper, we will present a model of the 3MR based on the properties of the total one-electron density distribution $\rho(r)$ and its associated Laplace field $\nabla^2\rho(r)$. In order to establish this model we will first analyze $\rho(r)$ and $\nabla^2\rho(r)$ for compounds CH_3X (X = CH_3, NH_2, OH, F) and CH_2X (X = CH_2, NH, O) along the lines developed in the preceding paper.[7] By extending these investigations to substituted **1** we will show that distortions of the valence sphere of C brought about by X can be rationalized in terms of a pronounced tendency of geminal and vicinal charge concentrations of avoiding each other. On the basis of this principle we will analyze concentration patterns in a variety of substituted **1** in order to derive rules describing the changes in $\rho(r)$, geometry, and stability of cyclopropane upon substitution. Special emphasis will be laid on the elucidation of the energetic consequences of ring,substituent interactions, in particular on the impact of a substituent on the strain and on the σ-aromaticity of cyclopropane, which has not been investigated so far. Finally, we will show that our model and, hence, the discussion of substituent effects apply to any molecular system with a topology similar to that of **1**.

II. Principle of Avoidance of Geminal and Vicinal Charge Concentrations

In an isolated atom with isotropically averaged one-electron density distribution $\rho(r)$ there are spherical surfaces where $-\nabla^2\rho(r)$ attains maximum or minimum value corresponding to local concentration or depletion of electronic charge. As has recently been shown by Bader and co-workers,[8] the Laplacian of ρ reflects the shell structure of an atom in the way that each quantum shell can be associated with a pair of shells of charge concentration and charge depletion. The uniform spheres of $-\nabla^2\rho(r)$, in particular the "valence sphere" of the Laplacian of $\rho(r)$ of an isolated atom, are distorted upon bond formation with other atoms. A pattern of maxima ("lumps") and minima ("holes") of $-\nabla^2\rho(r)$ emerges in the valence shell. Analysis of $-\nabla^2\rho(r)$ of simple molecules (Table I, Figure 1) reveals that distortions of these

(1) (a) Hoffmann, R. *Tetrahedron Lett.* **1970**, 2907–2909. (b) Hoffmann, R.; Stohrer, W.-D. *J. Am. Chem. Soc.* **1971**, *93*, 6941–6948. For a description of the relevant MOs see: Jorgensen, W. L.; Salem, L. "The Organic Chemist's Book of Orbitals"; Academic Press: New York, 1973.

(2) Günther, H. *Tetrahedron Lett.* **1970**, 5173–5176.

(3) For a recent review of experimental data, see: Allen, F. H. *Acta Crystallogr., Sect. B* **1980**, *B36*, 81–96. See also: Allen, F. H. *Acta Crystallogr., Sect. B* **1981**, *B37*, 890–900. Allen, F. H. *Tetrahedron* **1982**, *38*, 645–655. Allen, F. H.; Kennard, O. Taylor, R. *Acc. Chem. Res.* **1983**, *16*, 146–153.
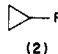
(4) (a) Skanche, A.; Boggs, J. E. *J. Mol. Struct.* **1979**, *51*, 267–274. (b) Skanke, A.; Boggs, J. E. *J. Mol. Struct.* **1978**, *50*, 173–182. (c) Skanche, A. *J. Mol. Struct.* **1977**, *42*, 235–240. (d) Skancke, A.; Boggs, J. E. *Acta Chem. Scand.* **1978**, *A32*, 893–894. (e) Hehre, W. J. *J. Am. Chem. Soc.* **1972**, *94*, 6592–6597. (f) Skancke, A. *Acta. Chem. Scand.* **1982**, *A36*, 637–639. (g) De Maré, G. R.; Peterson, M. R. *J. Mol. Struct.* **1982**, *89*, 213–225. (h) Durmaz, S.; Kollmar, H. *J. Am. Chem. Soc.* **1980**, *102*, 6942–6945. (i) Skancke, A.; Flood, E.; Boggs, J. E. *J. Mol. Struct.* **1977**, *40*, 263–270. (j) Oberhammer, H.; Boggs, J. E. *J. Mol. Struct.* **1979**, *57*, 175–182. (k) A classification of substituted cyclopropanes on the basis of MO theory was published after this work was finished: Clark, T.; Spitznagel, G. W.; Klose R.; Schleyer, P. v. R. *J. Am. Chem. Soc.* **1984**, *106*, 4412–4419.

(5) (a) Jason, M. E.; Ibers, J. A. *J. Am. Chem. Soc.* **1977**, *99*, 6012–6021. (b) Harmony, M. D.; Bostrom, R. E.; Hendrickson, D. K. *J. Chem. Phys.* **1975**, *62*, 1599–1600. See also: Harmony, M. D. *J. Chem. Phys.* **1978**, *69*, 4316–4318.

(6) (a) Deaknye, C. A.; Allen, L. C.; Craig, N. C. *J. Am. Chem. Soc.* **1977**, *99*, 3895–3903. (b) Deaknye, C. A.; Allen, L. C.; Laurie, V. W. *J. Am. Chem. Soc.* **1977**, *99*, 1343–1349.

(7) Cremer, D.; Kraka, E. *J. Am. Chem. Soc.*, preceding paper in this issue.

Table I. Description of Valence Spheres of Bonded Atoms in Terms of the Critical Points of $-\nabla^2\rho(r)^{a,b}$

molecule	critical point	$\rho(r)$	$-\nabla^2\rho(r)$	p_i^{ij} c	p_i^{ij}/p_i^{ik} d
	A. Distortion of Valence Sphere of Bonded C Atoms				
CH_3CH_3	l_C^{CC} (3,−3)	1.880	24.84	0.519	0.986
CH_3NH_2	l_C^{CN} (3,−3)	1.866	22.78	0.538	0.946
	l_N^{NC} (3,−3)	2.963	37.88	0.435	
	l_N^{nb} (3,−3)	4.007	79.76	0.387	
	(∠lNC: 108.1°; ∠lNH: 109.4°; ∠HCNl: 60°)				
CH_3OH	l_C^{CO} (3,−3)	1.856	18.37	0.557	0.903
	l_O^{OC} (3,−1)	4.645	53.97	0.374	
	l_O^{nb} (3,−3)	6.750	162.8	0.334	
	(∠lOC: 100.9°; ∠lOl: 140.6°; ∠HCOl: 73.4°)				
CH_3F	l_C^{CF} (3,−3)	1.773	10.52	0.557	0.898
	l_F^{FC} (3,−1)	3.878	−0.08	0.491	
	l_F^{nb} (3,−3)	10.560	284.2	0.293	
	(∠lFC: 99.7°; ∠lFl: 117.2°; ∠HCFl: 60°)				
▷—F **(2)**	l_1^{12} (3,−3)	1.930	26.33	0.507	0.737
	l_2^{21} (3,−3)	1.844	22.10	0.520	0.994
	l_2^{23} (3,−3)	1.808	21.34	0.523	
	B. Concentration Holes in Valence Sphere of Doubly Bonded Atoms *e*				
CH_2CH_2	l_C^{h} (3,+1)	0.987	−1.40	0.546	
CH_2NH	l_C^{h} (3,+1)	0.905	−2.39	0.555	
	l_N^{h} (3,+1)	2.187	6.17	0.442	
CH_2O	l_C^{h} (3,+1)	0.778	−3.38	0.574	
	l_O^{h} (3,+1)	4.205	28.22	0.373	
C_6H_6	l_C^{h} (3,+1)	1.132	−4.43	0.527	

a For definition of parameters see Table III of preceding paper.[7] l_X^{nb}: nonbonded concentration at X. Additional information about positions of nb concentrations is given in parentheses. *b* C//C calculations; only staggered conformations of CH_3XH_n are considered; geometry of **2** as described in text, CH_3XH_n and CH_2XH_m geometries from ref 17. *c* Valence sphere radius of isolated atoms; $p_C = 0.498$; $p_N = 0.441$; $p_O = 0.348$; $p_F = 0.301$.[8] *d* $p_i^{ik} = p_C^{CH}$; for **2** $p_i^{ik} = p_1^{14}$ and p_2^{23}, respectively. *e* Holes (h) are always above and below the plane forming an angle ∠hXh close to 180°.

spheres are such that concentration maxima, (3,−3) critical points, develop in the direction of the bond formed with an adjacent atom while saddle points, (3,−1) critical points, can be found between bonds. If the atom considered possesses electron lone pairs (lp), nonbonded charge concentration maxima will be found in a region which is usually assaigned to lp electrons.[8]

The pattern of the critical points of $-\nabla^2\rho(r)$ in the valence sphere of bonded atoms depicts some regularities which are best described by using the graph shown in Figure 1. If an atom A_i (e.g., C) is bonded to a strongly electronegative atom X_j (e.g., F), the valence sphere of A_i is pulled into the direction of X_j. This is revealed by the locations (l_i^{ij}) of the (3,−3) critical points (measured by distances p_i^{ij} [9]) and the values of $-\nabla^2\rho(r)$ at these points. The distortion of the valence sphere of A_i caused by X_j can be viewed as being the result of a charge transfer from A_i to X_j which is directly revealed by the fact that the minimum of $\rho(r)$ along the bond path moves toward A_i and a buildup of charge is found in front of X_j, shielding the nucleus of X_j in the direction of A_i.

While there are no constraints determining the changes in charge density upon bond formation, the corresponding changes in the Laplacian of $\rho(r)$ are always as such that they cancel within the boundaries of a bonded atom, i.e., $\nabla^2\rho(r)$ integrated over the subspace Ω defined by the zero-flux surface of $\rho(r)$ vanishes:[10]

$$\int_\Omega \nabla^2\rho(r)\,dr = \oint dS\,\nabla\rho(r)\cdot n = 0 \quad (1)$$

If there is a decrease of concentration at the (3,−3) critical point of A_i in the direction of X_j, an increase of concentration in the opposite direction can be expected on the basis of eq 1. This is confirmed when evaluating $-\nabla^2\rho(r)$ at positions l_i^{ik}, l_i^{il}, etc., and considering the corresponding distances p_i^{ik}, p_i^{il}, etc. (Figure 1b). In the way concentration of $\rho(r)$ expands and becomes more diffuse on one side of the atom, it contracts on the other side thus leading to a vanishing net effect of fluctuations in $\nabla^2\rho(r)$.

(8) Bader, R. F. W.; MacDougall, P. J.; Lau, C. D. H. *J. Am. Chem. Soc.* **1984**, *106*, 1594–1605.
(9) All parameters used in this work are defined in Table III of the preceding paper.[7]
(10) Bader, R. F. W. *J. Chem. Phys.* **1980**, *73*, 2871–2883.

a

b
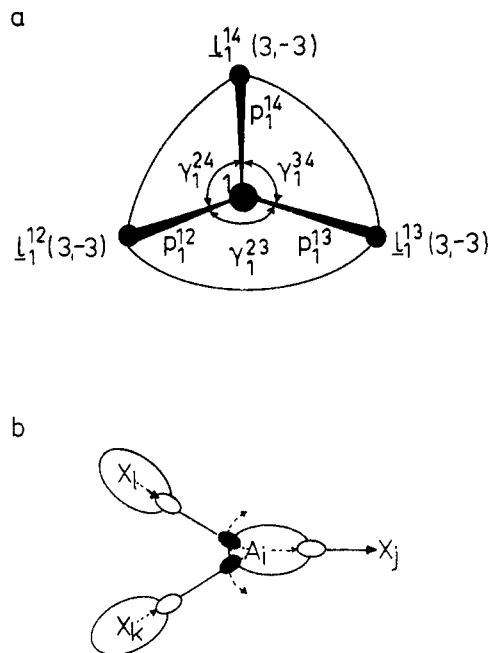
Figure 1. Description of the valence sphere of a bonded atom by the Laplacian of $\rho(r)$. (a) Atomic graph of $-\nabla^2\rho(r)$. Positions of nucleus (1) and concentration maxima l_i^{ij} are given. Distances p_i^{ij} and angles γ_i^{jk} determine the form of the atomic graph. (b) Distortion of the valence sphere of atom A_i caused by an electronegative atom X_j. The valence sphere is indicated by a large ellipsis. Small ellipses denote locations in the valence sphere where charge is compressed (solid) or expanded (open). The direction of distortions is given by dashed arrows. Propagation of distortion effects is shown for X_l and X_k.

Compression of density as revealed by $-\nabla^2\rho(r)$ shields nucleus A_i with regard to a second (or third) bonding partner X_k which is less electronegative than X_j. This interpretation is confirmed when analyzing the electron density in the bond region. The minimum of $\rho(r)$ along the bond path is shifted toward X_k, indicating the deshielding of this nucleus in the direction of A_i. The

Substituted Cyclopropanes, an Electron Density Model

J. Am. Chem. Soc., Vol. 107, No. 13, 1985   3813

a   b   c

Figure 2. Concentration of electron density in the lone-pair regions of F in CH_3F (HF/C//C calculations). Contour line diagrams have been drawn with regard to the plane that contains the F nucleus and is perpendicular to the CF bond axis. Positions of the methyl CH bonds are given by (heavy) dashed lines. (a) $\nabla^2\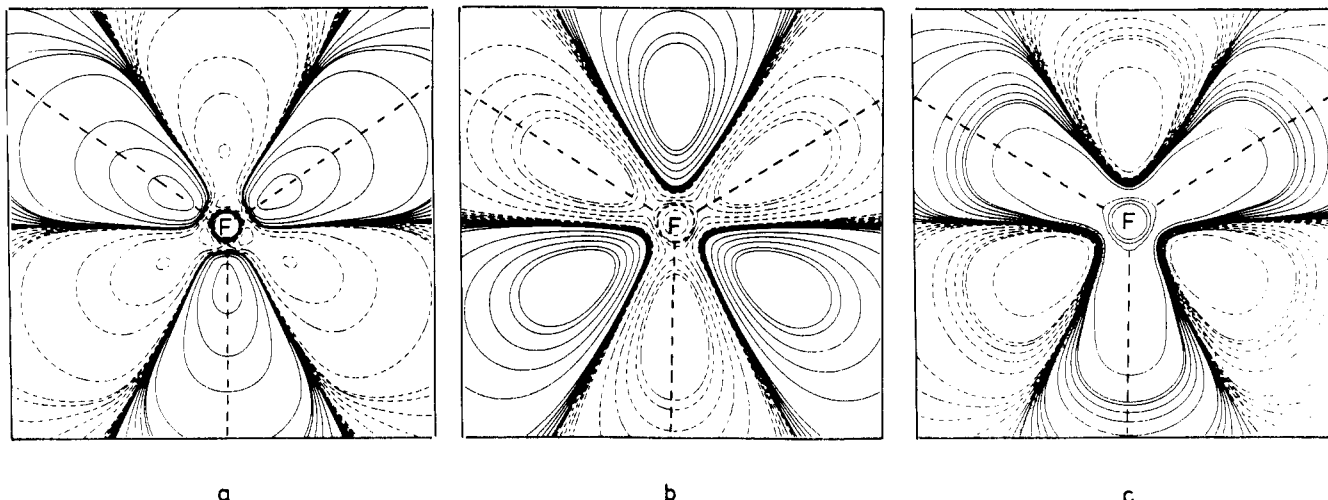rho(r)$; (b) $\rho(r)$; (c) $H(r)$. In order to amplify effects, difference maps are used, i.e., $\nabla^2\rho$, ρ, and H are plotted with regard to CH_3F with the methyl group rotated by 60° as reference. Dashed lines indicate areas with larger concentration (lower electron density; larger stabilizing energy density $(-H(r))$ and solid lines areas with smaller charge concentration (larger electron density, lower stabilizing energy density).

valence sphere of X_k is slightly pulled toward A_i as a reflection of the corresponding distortion of the valence sphere at A_i originally caused by X_j. In a chain of bonded atoms distortions can propagate to some extent to further atoms in the chain provided the electronegative character of X_j is the factor dominating the density distribution along the atom chain.

Analysis of the Laplacian of $\rho(r)$ in the valence sphere of a bonded atom leads to an insight into the electronic nature of its bonding partners. However, it has to be emphasized that distortions of the valence sphere are not obvious when considering $\rho(r)$ itself or $\nabla\rho(r)$. The strong exponential decay of $\rho(r)$ in the radial (off-nucleus) direction covers all local changes of the electron density around the nucleus. Thus, the Laplacian of $\rho(r)$ provides a means to disclose its *hyperfine structure*. Furthermore, the Laplacian of $\rho(r)$ connects features of the density distribution with energy properties via the local virial theorem:[10]

$$\frac{\hbar^2}{4m}\nabla^2\rho(r) = 2G(r) + V(r) \qquad (2)$$

where $G(r)$ and $V(r)$ are kinetic and potential energy densities, respectively. An increase of $|V(r)|$ leads to concentration of electronic charge at a point r, an increase of $G(r)$ to its depletion. A direct comparison of $G(r)$ and $V(r)$ according to eq 3[7] shows

$$H(r) = G(r) + V(r) \qquad (3)$$

that an electronegative atom X causes changes of the electronic energy $H(r)$ which are roughly parallel to those of $\nabla^2\rho(r)$, i.e., $H(r)$ becomes more (less) negative in those areas where the valence spheres of charge concentration contract (expand). The more (less) negative $H(r)$ is, the more is the electron density locally compressed (dilated) which in turn can be viewed in terms of shielding (deshielding) of the nucleus leading to a decrease (increase) of nuclear, nuclear repulsion, and smaller (larger) bond lengths.

In the way bond length changes are predicted from compression or expansion of the valence sphere, similar predictions can also be made with regard to bond angles. If, e.g., the valence sphere contracts, the angle γ between concentration points l_i^{ij} widens, revealing a marked tendency of geminal concentration lumps to avoid each other. This is indicated in Figure 1b.

The atomic graph derived from the pattern of critical points l_i^{ij} in the valence sphere of a bonded atom adopts a form which is directly related to features of the atomic graphs of neighboring atoms (Figure 1b). Besides the direct distortions of the valence sphere caused by an electronegative (electropositive) substituent X, vicinal charge concentrations being due to either bonded or nonbonded densities distort the valence sphere as well. If possible,

concentration lumps arrange in a way that again suggests a pronounced tendency to avoid each other. This is illustrated in Figure 2a where the Laplacian of $\rho(r)$ of CH_3F is plotted in a plane containing the F nucleus and being perpendicular to the CF bond. (To amplify effects the difference between $\nabla^2\rho(CH_3F)$ and $\nabla^2\rho(CH_3F$, rotated by 60° at the CF axis) is actually plotted.) At F there are three nonbonded concentration maxima forming an angle γ of 100° with the CF bond and being exactly staggered to the CH bond of the methyl group (see Table I).

This observation can be rationalized in the following way. In HF, the nonbonded charge concentration at the F atom adopts the form of a torus. If H is replaced by CH_3, the accumulation of electron density in the CH bonds causes a change of the potential, kinetic, and total energy densities in both the C–F bonding region and the valence sphere of F. Off-nucleus positions being staggered to the CH bonds do possess lower $V(r)$ and, hence, $H(r)$ values than those which are eclipsed (Figure 2c). Correspondingly, higher ρ-values are found at points with lower $H(r)$. This is illustrated by the difference density plot of the lp regions at the F atom of CH_3F (Figure 2b). The small variations of $\rho(r)$ in these regions have been determined by rotating the methyl group of CH_3F by 60° and comparing $\rho(r)$ thus obtained with the original density distribution. The preference for staggering of nonbonded charge concentrations is obvious from Figure 2 and has also been found for other molecules (Table I).

On the basis of the observations described above and the data collected in Table I we state that *geminal and vicinal bonded and nonbonded charge concentrations try to avoid each other*. This conclusion is not a trivial reformulation of the Coulomb law. One has to keep in mind that charge concentration and electron density are two different quantities. A priori, e.g., just by considering eq 2, there is no obvious way of deriving the principle stated above.

III. A Model of the 3MR Based on $\rho(r)$ and Its Laplace Concentration $\nabla^2\rho(r)$

The analysis presented above and in the preceding paper[7] suggests an electron density model for the description of substituent effects in cyclopropanes.

(1) The four concentration maxima in the valence sphere of the carbon atoms adopt positions such as to attain the best compromise between optimal directionality to the bonding partners and maximum avoidance of geminal charge concentrations in the valence sphere. In the case of cyclopropane, this compromise is achieved for concentrations l_c^{cc} at an angle γ of 92°. The directions of the bond paths are largely determined by the positions of the bonded charge concentrations. As a consequence bond paths are bent and cyclopropanes adopt convex-shaped molecular graphs.[7]
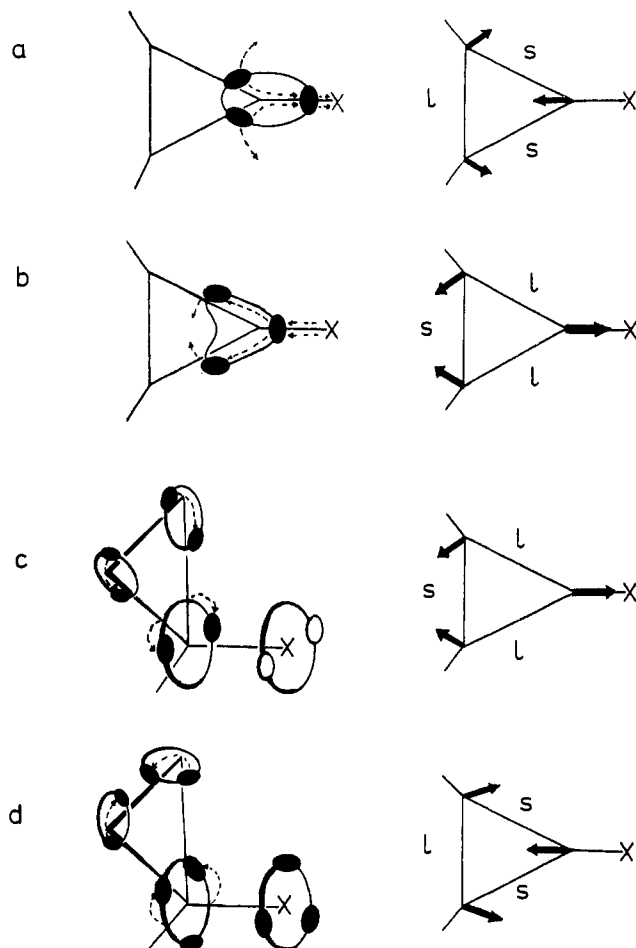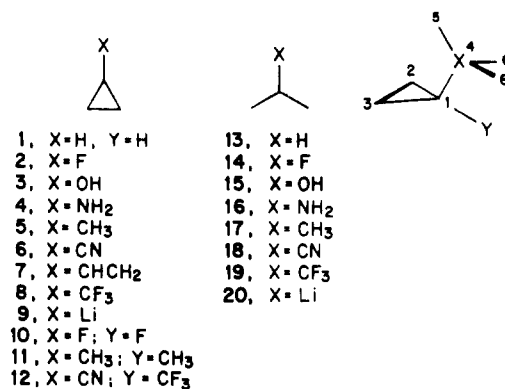
Figure 3. Distortions of the valence spheres of 3MR atoms (left side) by a substituent X with (a) σ-attractor, (b) σ-repeller, (c) π-attractor, and (d) π-repeller ability. Distorted valence spheres are indicated by (large) ellipses or circles. Small ellipses depict locations in the valence sphere or the bond region with charge compression (solid) or charge expansion (open). Dashed arrows indicate the direction of distortions of the valence spheres. 3MR nuclei move into the areas with charge compression as indicated by the heavy arrows in the diagram on the right side. The corresponding bond length changes are shown (s: small; l: long).

(2) Bonded concentrations at the substituted carbon atom of **1** are "pulled" into the direction of an electronegative substituent. In case of an electropositive substituent they are "pushed" toward the ring (see directions of the dashed arrows in Figure 3a,b). We call substituents pulling (pushing) concentration from (toward) the 3MR "σ-attractors" ("σ-repellers"). On the basis of the principle stated above the electronic impact of the substituent will lead to a change in γ. In the case of a σ-attractor γ will widen (due to avoidance of geminal concentration lumps), while γ will narrow in the case of a σ-repeller. The concomitant change of the length of the distal CC bond will be partially offset if the distortions of the valence sphere of C_1 are transmitted to the basal C atoms of the 3MR via the electron density in the bonding regions.

(3) A concentration buildup in the internuclear region leads to a screening of nuclear charges. Similarly, a compression of the valence sphere brought about by an electropositive bonding partner shields the nucleus. The nucleus is drawn into the region with charge accumulation and a shorter bond distance results. The reverse effect can be expected if the nucleus is deshielded due to charge depletion in the bonding region and due to an expansion of the valence sphere caused by an electronegative bonding partner. In Figure 3 (right side), changes in nuclear positions and overall geometry of the 3MR due to substituent effects on the electron density distribution are indicated by solid arrows.

(4) Lumps and holes in the valence sphere concentration of a substituent X lead to changes in the valence sphere of the adjacent

Chart I

1, X=H, Y=H   13, X=H
2, X=F   14, X=F
3, X=OH   15, X=OH
4, X=NH₂   16, X=NH₂
5, X=CH₃   17, X=CH₃
6, X=CN   18, X=CN
7, X=CHCH₂   19, X=CF₃
8, X=CF₃   20, X=Li
9, X=Li
10, X=F; Y=F
11, X=CH₃; Y=CH₃
12, X=CN; Y=CF₃

carbon atom. According to the principle of avoidance of charge concentrations, substituents possessing lumps in their valence spheres "push" density out of vicinal positions which are eclipsed to their lumps (Figure 3c,d left side; see also Figure 2). Vicinal lumps arrange such as to obtain maximum staggering. A substituent X with three lumps staggered to the C_1C_2, C_1C_3, and C_1H bond causes an increase of electron charge in these bonding regions. Density is pushed toward the basal C atoms, distorting their valence spheres as indicated in Figure 3d. Since C_1 is shielded against the basal C nuclei, bonds C_1C_2 and C_1C_3 become shorter while C_2C_3 lengthens due to a deshielding of C_2 and C_3 in the basal bond (Figure 3d, right side). Substituents possessing concentration holes in their valence spheres pull density in positions eclipsed with the locations of the holes. This causes a decrease of ρ in the C_1C_2 and C_1C_3 bond regions and therefore, enhanced repulsion between the corresponding nuclei. The valence spheres of the basal C atoms expand toward C_1 and contract in the C_2C_3 bond region leading to a decrease of nuclear repulsion between the basal C nuclei. The geometrical changes indicated in Figure 3c (right side) result. In order to distinguish between the various effects of a substituent on vicinal charge concentrations we speak of "π-repeller" (Figure 3d) and "π-attractor" substituents (Figure 3c), where the prefix π indicates that the influence of the substituent is not transmitted through the bond path. (For example, in CH_3F the ellipticity at $r_b(CF)$ is 0, i.e., ρ is isotropically distributed at the bond critical point.)

Utilizing the electron density model outlined above and in Figure 3, substitutent, ring interactions in cyclopropanes **1–12** shown in Chart I are now investigated in detail. For this purpose, the following procedure has been applied. First, 6-31G* (basis C) calculations have been carried out by using the calculated 4-31G (basis B) geometry of **1** and standard values for the substituent geometry.[11] Conformations at the C_1X bond have been chosen as to allow maximum staggering of bonds and to preserve C_s symmetry of the 3MR. The density distribution $\rho(r)$ obtained at this level has been analyzed with the aid of its associated Laplace field $\nabla^2\rho(r)$, whereas special emphasis has been laid on the distortions of the valence spheres of the ring atoms caused by the substituent X. These distortions become obvious when comparing $\nabla^2\rho$-values, distances p_i^{ij}, and angles γ_i at positions l_C^{cc} (for a description of parameters see Table III of the preceding paper[7]). As an example, calculated features of the valence spheres of the heavy atoms of fluorocyclopropane (**2**) are given in Table I. They reveal both the strong σ-attractor ability of F (see, e.g., ratio p_1^{12}/p_1^{14}) and its π-repeller character (ratio $p_2^{21}/p_2^{23} < 1$, see also Figure 4). A shortening of the vicinal and a lengthening of the basal CC bond can be predicted (Figure 4). Compared to **1**, there are, however, only small changes with regard to l_C^{CH} charge concentrations, suggesting that geometries of CH_2 groups are hardly influenced by the substituent.

In the second step of the investigation, predictions made on the basis of valence shell distortions for standard geometries of **1–12**

---

(11) Standard geometries: Pople, J. A.; Gordon, M. S. *J. Am. Chem. Soc.* **1967**, *89*, 4253–4261. 4-31G and 6-31G* basis: see ref 15 in ref 7.

Table II. Calculated Energies and Geometries of Substituted Cyclopropanes and Propanes[a]

| | | energies | | geometry | | | |
	molecule	basis B (4-31G)	basis C (6-31G*)	$R(C_1C_2)$ vicinal	$R(C_2C_3)$[b] distal	∠(CC)CX	∠XCY
			A. Cyclopropanes				
1, X = H; Y = H[c]		−116.88385	−117.05871	1.502			
2, X = F		−215.61002	−215.90539	1.484	1.512	122.6	113.3
3, X = OH		−191.62039	−191.90154	1.492	1.516	127.5	109.7
4, X = NH₂		−171.82271	−172.08107	1.496	1.502	121.4	116.8
5, X = CH₃		−155.86341	−156.09500	1.502	1.508	125.6	113.8
6, X = CN		−208.47609	−208.79316	1.511	1.493	124.2	113.3
7, X = CH=CH₂[d]		−193.65282	−193.93764	1.522	1.510	125.1	115.2
8, X = CF₃		−452.07873	−452.67954	1.498	1.498	124.5	111.3
9, X = Li		−123.70042	−123.87707	1.533	1.501	124.9	120.2
10, X = F; Y = F		−314.34502	−314.76262	1.465	1.532	125.4	109.2
11, X = CH₃; Y = CH₃		−194.84301	−195.13127	1.504	1.504	122.9	114.2
12, X = CN; Y = CF₃		−543.65954	−544.40340	1.513	1.488	123.1	113.4
			B. 2-Propanes				
13, X = H[e]		−118.09363	−118.26357	1.529	112.5	126.8	106.4
14, X = F		−216.82749	−217.11845	1.516	113.4	127.4	106.6
15, X = OH		−192.83809	−193.11449	1.523	112.7	126.1	103.8
16, X = NH₂		−173.03162	−173.28505	1.524	111.5	125.1	111.2
17, X = CH₃		−157.07197	−157.29841	1.532	110.8	123.4	107.9
18, X = CN		−209.68378	−209.99595	1.537	111.7	124.7	106.9
19, X = CF₃		−453.28970	−453.88434	1.529	112.2	126.6	105.1
20, X = Li		−123.57033	−125.06899	1.547	109.2	132.6	106.9

[a] Energies in hartree, distances in Å, angles in deg, CX bond length for **9** and **20** = 1.945 Å. [b] For 2-propanes angle ∠$C_1C_2C_3$ is given. [c] $R(CH)$ = 1.071 Å; ∠HCH = 113.8°. [d] From ref 4a. [e] ∠(HH)C_1C_2 = 127.1°; ∠HC_1H = 107.6; ∠HC_1C_2 = 111.6.

Table III. Description of 3MR Bonds in Terms of Energy and Density[a]

parameter	1 X, Y = H, H	2 F	3 OH	4 NH₂	5 CH₃	6 CN	7 CH=CH₂	8 CF₃	9 Li	10 F, F	11 CH₃, CH₃	12 CN, CF₃
n_1	1.000	1.107	1.075	1.042	1.011	0.968	0.916	1.011	0.891	1.216	1.016	0.963
n_2		0.967	0.957	0.997	0.983	1.036	0.943	1.014	1.001	0.919	0.988	1.056
$-\nabla^2\rho_{b,1}$	12.63	15.21	14.51	13.68	12.93	11.96	11.74	12.81	10.07	17.87	13.00	11.87
$-\nabla^2\rho_{b,2}$		11.77	11.64	12.49	12.27	13.64	12.39	12.98	12.85	10.61	12.39	14.14
$-H_{b,1}$	1.439	1.626	1.566	1.514	1.459	1.394	1.353	1.465	1.277	1.837	1.465	1.405
$-H_{b,2}$		1.381	1.362	1.438	1.411	1.507	1.402	1.468	1.442	1.290	1.422	1.543
$R_{b,1}$	1.511	1.497	1.505	1.508	1.513	1.520	1.531	1.508	1.540	1.484	1.516	1.523
$R_{b,2}$		1.521	1.525	1.510	1.516	1.503	1.520	1.508	1.510	1.539	1.513	1.498
β_1	78.9	84.9	83.0	82.4	80.3	80.1	77.9	81.5	72.3	94.4	81.4	82.6
β_2		79.4	79.9	79.0	79.2	77.8	79.3	78.2	79.2	78.5	79.4	77.0

[a] For definition and dimension of parameters see Table III of preceding paper.[7] C/HF//B calculations.

Table IV. Description of Valence Spheres of 3MR Atoms by the Critical Points of $-\nabla^2\rho(r)$[a]

critical point	parameter	1 X, Y = H, H	2 F	3 OH	4 NH₂	5 CH₃	6 CN	7 CH=CH₂	8 CF₃	9 Li	10 F, F	11 CH₃, CH₃	12 CN, CF₃
l_1^{12}	$-\nabla^2\rho$	21.33	27.45	25.31	23.83	21.74	22.42	20.51	22.96	15.52	34.08	22.09	23.79
(3, −3)	ρ	1.805	1.980	1.915	1.877	1.818	1.840	1.768	1.868	1.607	2.158	1.825	1.888
	ρ_1^{12}/ρ_1^{14}		0.735	0.865	0.959	1.008	0.963	1.110	0.975	1.116	0.909	1.006	0.969
	γ_1	91.8	96.1	94.5	94.4	92.8	92.2	91.3	95.8	87.8	102.3	93.8	97.1
l_2^{21}	$-\nabla^2\rho$		23.26	23.39	22.14	21.86	19.01	20.42	20.30	20.79	24.74	22.17	17.90
(3, −3)	ρ		1.897	1.894	1.845	1.831	1.723	1.767	1.779	1.773	1.965	1.844	1.688
	ρ_2^{21}/ρ_2^{23}	1.000	0.944	0.988	0.998	0.994	1.021	1.000	1.009	0.986	0.992	0.992	1.031
l_2^{23}	$-\nabla^2\rho$		20.38	20.20	21.07	20.80	22.42	20.97	21.68	21.22	19.35	20.85	23.00
(3, −3)	ρ		1.769	1.760	1.799	1.788	1.847	1.787	1.822	1.806	1.721	1.791	1.869
	γ^2		91.8	92.4	91.8	92.1	92.0	91.9	91.2	92.8	91.5	92.2	90.4
l_4^{45}; l_4^{nb}	$-\nabla^2\rho$		280.0[b]	23.59[b]	79.28	28.66	1.69[b]	31.44	15.01		276.9	28.69	2.12[b]
(3, −3)	ρ		10.506	3.145	3.987	1.987	1.080	2.061	1.832		10.454	1.988	1.117
trans	p		0.293	0.544	0.388	0.511	0.528	0.506	0.531		0.294	0.512	0.524
	θ		100.2	108.4	107.1	108.8	76.3	118.2	111.6		100.3	108.8	73.6
	τ		52.3	52.8	51.3	51.8	51.7	50.9	52.1		56.7	51.8	53.6
l_4^{46}; l_4^{nb}	$-\nabla^2\rho$		284.9	164.1	46.70	28.91	0.89[c]	1.32[c]	15.35		289.2	28.77	0.88[c]
(3, −3)	ρ		10.56	6.75	3.18	1.993	1.038	0.982	1.840		10.61	1.990	1.054
gauche	θ		99.8	100.3	107.5	109.0	78.0	76.8	111.5		99.8	109.0	76.6
	τ		49.5	53.5	70.9	68.2	36.1	16.5	67.9		38.6	68.3	34.4

[a] For definition of parameters, see Table III of preceding paper.[7] C/HF//B calculations. nb: nonbonded charge concentration; position 5 is trans, position 6 is gauche with regard to the C_1Y bond (see Chart I); θ denotes the angle ∠lX_4C_1, τ is the dihedral angle $lX_4C_1l_1^{12}$; angles $l_4^{45}X_4C_1C_2$ are smaller, angles $l_4^{46}X_4C_1C_2$ are larger by 16–18°. [b] (3, −1) critical point. [c] (3, +1) critical point.

have been used to carry out a partial optimization of the 3MR with basis B. In all cases, computed geometries confirm the predicted changes of the 3MR bonds. Reinvestigation of $\rho(r)$ and its changes due to geometry optimization substantiates the density model developed above and provides additional insight into ring, substituent interactions. In order to discuss these interactions in more detail, energies, geometries and electron density features of compounds **1–12** computed at the C/HF//B level of theory

Table V. π-Character of 3MR Bonds and Degree of Surface Delocalization[a]

	molecule					direction[b]		
	X	Y	ϵ_1	ϵ_2	ϵ_r	of v_r^2	ρ_r	η
1	H	H	0.483		0	no	1.364	81.9
2	F		0.429	0.531	0.091	⊥	1.391	80.4
3	OH		0.410	0.518	0.117	⊥	1.367	80.7
4	NH$_2$		0.487	0.512	0.043	⊥	1.385	81.6
5	CH$_3$		0.456	0.499	0.051	⊥	1.360	80.9
6	CN		0.530	0.395	0.196	‖	1.355	82.0
7	CH=CH$_2$		0.486	0.449	0.025	‖	1.322	81.6
8	CF$_3$		0.480	0.448	0.085	‖	1.374	81.3
9	Li		0.478	0.467	0.007	‖	1.337	84.7
10	F	F	0.332	0.579	0.162	⊥	1.389	78.4
11	CH$_3$	CH$_3$	0.444	0.493	0.064	⊥	1.361	81.3
12	CN	CF$_3$	0.541	0.357	0.309	‖	1.356	80.8

[a] For definition of parameters see Table III in preceding paper.[7] C/HF//B calculations. [b] Direction of the major axis of ϵ_r is either parallel (‖) or perpendicular (⊥) to the basal CC axis.

are summarized in Tables II–V.

Fluoro-, Hydroxy-, and Aminocyclopropanes (2, 3, 4). A σ-attractor substituent should lead to the density and concentration pattern sketched in Figure 3a. As a result the basal CC bond should be lengthened accompanied by a decrease of the vicinal bonds. If the substituent is not only a σ-attractor but also a π-repeller as in the case of F, OH, etc., changes in the valence sphere of C$_1$ due to avoidance of vicinal charge concentrations will amplify those caused by the σ-attractor ability of the substituent. Since a π-repeller leads to an increase of $\rho(r)$ and $-\nabla^2\rho(r)$ in the vicinal cyclopropane bonds, the valence spheres of C$_2$ and C$_3$ are compressed on the side of the charge buildup but expand in the basal CC bonds. In this way, the π-repeller effect of the substituent leads to the bond changes shown in Figure 4a.

Contrary to CH$_3$F, nonbonded charge concentrations at the F atom of **2** are no longer perfectly staggered with regard to the vicinal bonded concentrations. There are two gauche oriented concentration maxima in a line parallel to the basal CC axis. With the F nucleus they form an angle 33° greater than the one found for CH$_3$F (117°, Table I). Obviously, the two geminal F concentrations gauche to the C$_1$H bond avoid each other as far as possible. At the C$_1$ atom they push density into the vicinal CC bonds which is reflected to some extent by the concentration and density values at l_1^{24} (l_1^{34}): $-\nabla^2\rho(r) = 0.08$; $\rho = 1.203$ (for **6** these values are 6.10 and 1.379). In addition, density is pushed out of the region between the vicinal 3MR bonds due to the nonbonded F concentration at F trans to the C$_1$H bond (Figure 4). The resulting changes in $\rho(r)$ provide a rationalization for calculated n, $\nabla^2\rho_b$ and H_b values of **2** (Table III). Predictions made in the preceding section with regard to CC bond length changes are fully confirmed by the relevant data of Table II.

When exchanging the F substituent by a hydroxy or an amino group both the σ-attractor ability of the heteroatom and the π-repeller effect arising from bonded XH or nonbonded charge concentrations at X decrease (see relevant data at l_4^{45} and l_4^{46} in Table IV). The latter decrease is due to an increase of the CX bond length and a decrease of the concentration maxima at X (Table IV). As a consequence, distortions of valence spheres are less pronounced but still yield vicinal CC bonds shorter than the basal CC bond (Tables II and III).

It is interesting to note that in the case of the hydroxy substituent both the calculated distal and the vicinal CC bonds of the 3MR (**3**) are longer than might be expected from the corresponding values of **2** and **4**. We tentatively explain this result with the fact that a positively charged H atom resides above the 3MR of **3** thus attracting electronic charge from the ring area. In this way, electron density is removed to some extent from the 3MR bonds, leading to the observed weakening of the three CC bonds. Similar second-order effects should be caused by other substituents with positively charged atoms in an endo position (above the ring) while negatively charged atoms should push density from the interior of the ring into the 3MR bonds thus strengthening them (see Figure 5a,b).

a

b
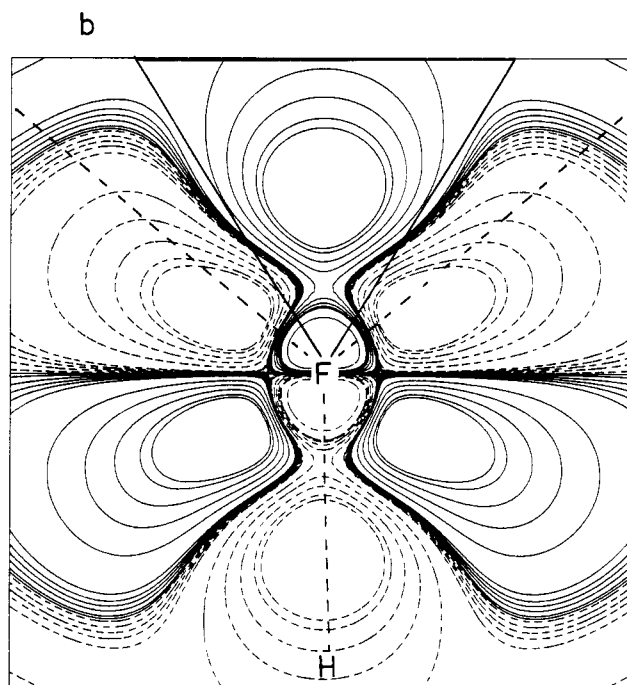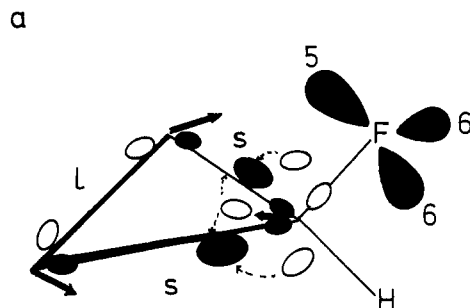
Figure 4. Fluorocyclopropane (**2**): (a) Qualitative description of valence sphere distortions of 3MR atoms by nonbonded concentrations of F (5, 6, 6'). Compare with Figure 3. (b) Difference density map of $\rho(r)$ for **2** with regard to the plane containing the F nucleus and being perpendicular to the bond C$_1$F. For more details see Figure 2. (Dashed lines (heavy) indicate the directions given by vicinal bonded charge concentrations. Note the deviation from internuclear axes of 3MR (solid lines).)

The interpath angles of the 3MR show the expected dependency on the electronic nature of the substituent. A σ-attractor (σ-repeller) substituent increases (decreases) the angle β_1 which can be rationalized in terms of the distortions of the valence sphere of C$_1$ and the principle of avoidance of geminal bonded charge concentrations. Angles β_2 and β_3 remain fairly constant (79 ± 1°) when X is varied. Investigation of $\Delta\beta_i^{ij}$ reveals that this is actually a result of mutual cancellation of larger changes in increment angles $\Delta\beta_2^{21}$ and $\Delta\beta_2^{23}$.

Cyanocyclopropane (6). Any 3MR model suggested as an alternative to the Walsh model should prove its usefulness by predicting bond length changes caused by π-acceptor substituents like the CN group. In terms of $\rho(r)$ and $\nabla^2\rho(r)$ such a substituent is a π-attractor (Figure 3c). The C atom of the CN group possesses in its valence sphere two holes, (3,+1) critical points of $-\nabla^2\rho(r)$, which are positioned on a line exactly parallel to the basal C$_2$C$_3$ axis. Accordingly, density is pulled out of the vicinal CC bonds into interbond positions of the valence sphere of C$_1$. The valence spheres at the basal C atoms expand into the C$_1$C$_2$ and C$_1$C$_3$ bond regions but contract in the C$_2$C$_3$ bond region. Deshielding and shielding areas can be distinguished, and shortening (lengthening) of the basal (vicinal) bond(s) of the 3MR
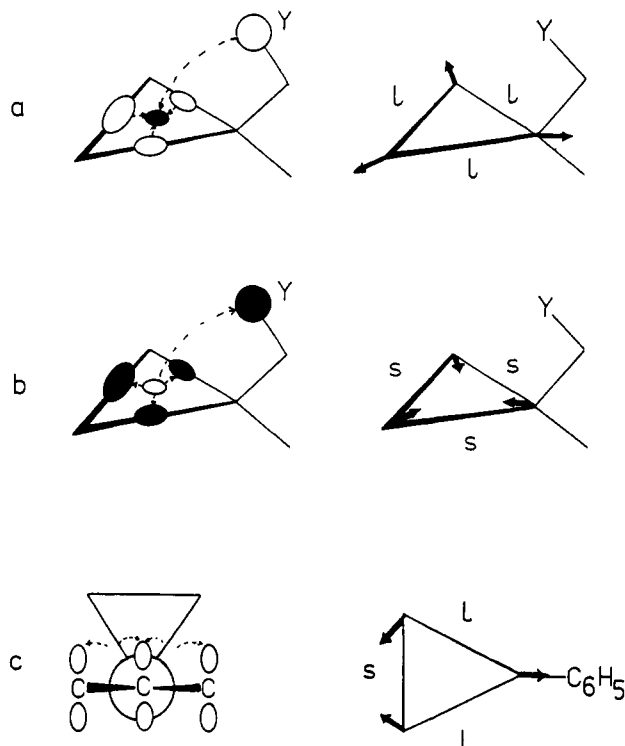
Figure 5. Geometrical changes of the 3MR (right side) caused by secondary effects of a substituent Y (bonded to X) with attractor (a) or repeller ability (b). Changes in concentration in the bonded regions of the 3MR are shown on the left side schematically by small ellipses (solid ellipse, increase of concentration; open ellipse, decrease of concentration). (c) Influence of a perpendicular phenyl substituent on the bonded concentrations of cyclopropane. A Newmann projection along the C_4C_1 bond is shown on the left side. Concentration holes at C_4 and its neighboring atoms in the phenyl ring are indicated by small open ellipses. Dashed arrows indicate the direction of distortion of bonded charge concentrations in the 3MR.

can be predicted (Figure 3c). The calculated bond lengths (1.493 and 1.511 Å) are in line with these predictions.

Lithiocyclopropane (9). In general, a σ-repeller substituent will cause a lengthening of the vicinal CC bonds and a shortening of the distal CC bond (Figure 3b). For strong σ-repellers, the latter effect will be partially or even totally offset if the distortions of the valence sphere of C_1 are transmitted to the basal C atoms thus leading to deshielding of nuclei C_2 and C_3. The data of Table IV (e.g., p_2^{21}/p_2^{23}) and the calculated bond lengths of 9 (Table II) suggest that this is true for X = Li and the cyclopropyl anion discussed in the preceding paper.[7] For X = BeH, BH_2, etc., distortions of the valence spheres of C_2 and C_3 should decrease and the effect shown in Figure 3b should prevail.

Methyl-, Vinyl-, and (Trifluoromethyl)cyclopropane (6, 7, 8). These substituents produce relatively small changes in the electronic structure of 1, which are difficult to predict on the basis of the Walsh model. The distortions of the valence sphere of C_1 brought about by substituent X (Table IV) suggest that CH_3 is both a weak σ- and π-repeller, vinyl a weak σ-repeller, and π-attractor, and CF_3 a σ-attractor and a π-repeller. In addition, all three substituents can influence the density in the ring by secondary effects since they possess positively or negatively charged atoms which reside above the ring plane. Therefore, ring bonds of 6 and 7 should be longer (see Figure 5a) and those of 8 shorter (see Figure 5b) than those of 1. This is confirmed by the calculated geometries (Table II). Also, the variation in the ring bond lengths is in line with the predictions made for a π-attractor (7; Figure 3c) and a π-repeller (6, 8; Figure 3d). It is noteworthy that the actual differences in the CC bonds of 8 only become apparent if $\rho(r)$ and $H(r)$ are analyzed (Table III). The calculated bond lengths are equal in this case.

Difluoro-, Dimethyl-, and Methylcyanocyclopropane (10, 11, 12). The calculated density and concentration properties suggest

Table VI. Stability of Substituted 3MRs and 2-Propanes Given Relative to Cyclopropane and Propane[a]

molecule	$\Delta E(I)^b$	ΔSE^c	ΔDE^d	molecule	$\Delta E(III)$
1 X = H	0	0	0	13 X = H	0
2 X = F	−5.1	−9.2	−15	14 X = F	9.7
3 X = OH	−5.0	−8.4	−13	15 X = OH	7.6
4 X = NH_2	0.6	−5.1	−4	16 X = NH_2	5.2
5 X = CH_3	1.0	−2.9	−1	17 X = CH_3	1.3
6 X = CN	1.3	1.5	3	18 X = CN	1.1
8 X = CF_3	0.1	0	0		
9 X = Li	6.1	9.6	16	20 X = Li	−8.9

[a] All values in kcal/mol. [b] Energy of reaction II for **1** is −26.7 kcal/mol (C//B calculations). Positive values are indicative of a stabilizing influence of the substituent, i.e., a decrease of the CSE of **1**. [c] Strain energies calculated by utilizing interpath angles β_i (Table III) and a CCC bending force constant of 1.071 (mdyn·Å)/rad².[12] Reference value is 75 kcal/mol (**1**). Positive ΔSE values indicate an increase in strain relative to **1**. [d] Delocalization energies estimated from $\Delta E(I)$ and SE values. Reference value is 48 kcal/mol (**1**). Positive ΔDE values indicate an increase in DE relative to **1**.

that the electronic effects of the individual substituents are not always additive. This holds only for the F atoms where the nonbonded concentrations have to adopt positions which amplify the π-repeller effect of one F substituent. In **11**, however, both the σ- and π-repeller effects of one methyl group are cushioned. The H atoms of the methyl groups which are in close contact with each other transfer less charge to the C atoms in order to avoid destabilizing electrostatic repulsion. As a consequence, the methyl C atoms neither push nor pull charge concentrations to or from C_1. The secondary effects of the H atoms above the ring plane prevail thus leading to an overall lengthening of the 3MR bonds (Figure 5a).

For **12** a dominance of π-attractor effects of the CN group is observed, i.e., the π-repeller effect of the CF_3 group does not change the density and concentration pattern of compound **6** significantly. This has to do with the fact that the concentration holes at the CN carbon are in positions exactly parallel to the basal CC axis and in addition much closer to the C_1 valence sphere than the bonded CF concentrations of the CF_3 group.

IV. π-Character of 3MR Bonds, Surface Delocalization of Electrons, and Energetic Consequences of Cyclopropane Substitution

A substituent at C_1 can change the ability of a cyclopropane ring to act as a conjugate group in a cyclopolyene. If the basal CC bond is incorporated into the framework of a conjugated system (**21a, 21b**) π-repeller substituents (F, OH, etc.) will
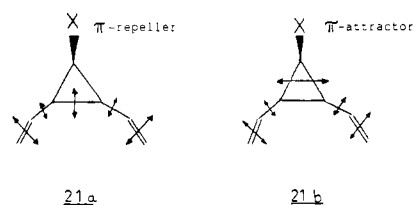
facilitate and π-attractor substituents (CN, $CH{=}CH_2$, etc.) will impede π-conjugation. This is suggested by the calculated bond ellipticities ϵ_b^9 of **1–12** (Table V) which describe the π-character of the cyclopropane bonds.[7]

The preferential direction of surface delocalization is given by the major axis of the ring ellipticity ϵ_r.[7] It points always to the CC bond(s) with the largest π-character, i.e., it is perpendicualr to the basal CC bond for X being a σ-attractor or π-repeller substituent while it is parallel for σ-repeller and π-attractor substituents (Table V).

The degree of surface delocalization as determined by the ratio $\eta = \rho_r/\bar{\rho}_b^7$ is largest for **9**. Electron density is more uniformly distributed in the 3MR plane in the case of X = Li (**9**) than for X = F (**2**). The data of Table V suggest that a strong π-repeller like F leads to a decrease of surface delocalization and σ-aromaticity of **1** while a strong σ-repeller like Li has the reverse effect.

Table VII. Substituent Effects on Geometry and Stability of Cyclopropanes[a]

type of substituent	example	C_1C_2 (vicinal)	C_2C_3 (distal)	strain energy	σ-aromaticity	stability of 3MR
σ-attractor	b	shorter	longer	decrease	decrease	decrease
σ-repeller	Li, BeH	longer	shorter[c]	increase	strong increase	increase
π-attractor						
bisected	CN, CHO	longer	shorter	(increase)	(increase)	negligible
perpendicular	C_6H_5	(longer)	(shorter)			
π-repeller	F, OH	shorter	longer	decrease	strong decrease	decrease

[a] Changes are given relative to cyclopropane. [b] A pure σ-attractor has not been found in this work although F, OH, etc., possess besides their π-repeller ability σ-attractor properties. [c] A strong σ-repeller leads to a distortion of the valence spheres of the basal C atoms as described in section III. A longer distal bond results. Compare with the cyclopropyl anion in ref 7.

Judging from calculated interpath angles β_i (Table III), a π-repeller substituent causes a decrease in the ring strain of **1**. If the CCC bending force constant $(1.071 \text{ mdyn Å/rad}^2)^{12}$ is used in connection with β values, a decrease of 9 kcal/mol is calculated for **2** (X = F). Since both surface delocalization and ring strain are reduced in this case it is difficult to predict which effect prevails. In order to make a valid assessment of the net effect on the stability of the 3MR, we have evaluated the energy of the formal reaction I, $\Delta E(\text{I})$. Since the energy of the homodesmotic reaction II provides a reasonable estimate of the conventional strain energy (CSE) of substituted **1**,[13] $\Delta E(\text{I})$ describes the change in CSE of **1** upon substitution.

$$\text{(I)}$$

$$\text{(II)}$$

Calculated values of $\Delta E(\text{I})$ are given in Table VI. They suggest that strongly electronegative substituents like F and OH increase the CSE of **1** while strongly electropositive substituents (e.g., Li) decrease the CSE of **1**. For X = NH_2, CH_3, CN, or CF_3 only moderate changes in CSE(**1**) are predicted although some of these substituents lead to appreciable changes in the 3MR geometry. This observation, however, is in line with thermochemical measurements on **4–6**.[13a] We consider the small changes in the CSE found in these cases as the net effect of two conflicting factors, namely ring strain and σ-aromaticity (surface delocalization) of the 3MR. Bending strain increases in the series **2, 3, 4, 5, 1, 6, 9**, as is suggested by the interpath angles β_1 and β_2 (see Tables III and VI). Parallel to this destabilization a stabilizing increase of surface delocalization can be expected (vide infra), its energetic influence outweighting the increase in strain in the case of **9** (Table VI).

While the determination of strain and delocalization energies may be a matter of disbute, the calculated variation of energy and electron density properties of compounds **1–12** provides sufficient support for the description of substituent effects on ring strain and surface delocalization outlined above. In those cases where a comparison is possible the CSE values given in Table VI are in line with the few scattered data on the stability of substituted **1** published in the literature.[13a]

V. Predictive Power of the Electron Density Model

A number of predictions can be made by applying the principles developed in this work (see Table VII):

(a) 3MR substituents like –HC=CHR, –phenyl, –N≡C, –C≡N, –NO_2, –RC=O, etc., are potential π-attractors since they possess a concentration hole, i.e., a (3,+1) critical point of $-\nabla^2\rho(r)$ in the valence sphere of the atom bonded directly to the 3MR (see Table I). If the concentration holes are aligned parallel to the basal CC axis (bisected conformations), a shortening of the basal

and a lengthening of the vicinal bonds should be observed (Figure 3c). These effects can be enhanced by a potential σ-attractor ability of X.

It is interesting to note that in those cases where the substituent X prefers for steric reasons a perpendicular rather than a bisected conformation, its π-attractor ability should persist. This is illustrated in Figure 5c for X = phenyl. The concentration holes at C_4 (as well as those at the ortho-C atoms of phenyl) pull charge concentration out of the vicinal bonds of the 3MR. Consequently, similar bond changes as in the bisected conformation should be observed. Experimental observations are in line with this prediction.[3]

(b) Halogens like F, Cl, and Br, alkoxy groups, and amino groups are sufficiently strong π-repellers. They should always cause an increase of the basal and a decrease of the vicinal bonds.

(c) Most interesting are σ-repeller substituents like Li, BeR, etc., which may lead to peculiar 3MR properties due to an increase of surface delocalization and σ-aromaticity of **1**. They cause a lengthening of the vicinal bonds and a shortening (lengthening) of the distal bond, depending on their (large) repeller ability.

(d) No example of pure σ-attraction is given in this work. Although a substituent like F possesses σ-attractor ability, our analysis suggests that its π-repeller character prevails.

(e) In polysubstituted cyclopropanes substituent effects will only add if there are no primary interactions between substituents which may cushion their original impact on the 3MR. This is mostly the case for geminal substituents while vicinal substituents should be additive in their effects.[3]

Point e will be of particular interest if **1** is incorporated in a polyene (**21**). The π-attractor effects of the two double bonds superimpose in the 2,3 bond thus enhancing its π-character and facilitating π-conjugation. This will be of relevance in a cyclic system like norcaradien (**22a**) or tricyclo[4.4.1.0^{1,6}]undeca-2,4,7,9-tetraene (**23a**). The parent compounds are known to be

22   23

a, R = H
b, R = CN

unstable[14] and therefore exist preferentially in their more stable valence tautomeric forms, namely cycloheptatriene and 1,6-methanol(10)annulene. It has been shown that the norcaradiene forms can be obtained in the form of the CN substituted derivatives **22b** and **23b**.[15] Since CN both strengthens the 1,6 bond in **22** (**23**) and increases the overall stability of the 3MR system slightly, valence tautomeric equilibrium between **22** (**23**) and its open counterpart is shifted toward the norcaradienic forms. Similar considerations can be made for other substituents and we will come back to this point in another paper.[16]

(12) Snyder, R. G.; Zerbi, G. *Spectrochim. Acta* **1967**, *23A*, 391–437.

(13) (a) Fuchs, R.; Hallman, J. H.; Perlman, M. O. *Can. J. Chem.* **1982**, *60*, 1832–1835. (b) Dill, J. D.; Greenberg, A.; Liebman, J. F. *J. Am. Chem. Soc.* **1979**, *101*, 6814–6826. (c) Greenberg, A.; Liebman, J. F.; Dolbier, W. R.; Medinger, K. S.; Skancke, A. *Tetrahedron* **1983**, 1533–1538.

(14) Cremer, D.; Dick, B. *Angew. Chem., Int. Ed. Engl.* **1982**, *21*, 865–866.

(15) (a) Ciganek, E. *J. Am. Chem. Soc.* **1965**, *87*, 652–653. (b) Vogel, E.; Scholl, T.; Lex, J.; Hohlneicher, G. *Angew. Chem., Int. Ed. Engl.* **1982**, *21*, 866–867.

Structural and energetic predictions for substituted **1** are summarized in Table VII. They can be extended to molecules with a topology similar to that of **1**. A prime example is propane. Analyzing $\rho(r)$, $\nabla^2\rho(r)$, and $H(r)$ of 2-propanes **13–20** (Table II) in the same way as cyclopropanes **1–12**, similar predictions with regard to CC bond length changes upon substitution of **13** can be made. Geometry optimization of **13–20** confirms these predictions (Table II), showing that π-repellers shorten and σ-repellers and π-attractors lengthen vicinal bonds. The actual effects are smaller than those observed for **1–12** which has to do with the fact that all nuclei are well shielded in the propanes with the bond paths almost coinciding with the internuclear axes. The energetic effect of the substituent on propane can be measured with the energy of the formal reaction III. The calculated values (Table

$$CH_3CHXCH_3 + CH_4 \rightarrow CH_3CH_2CH_3 + CH_3X \quad (III)$$
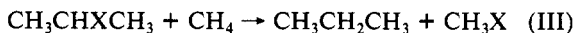
VI) show an increase in stabilizing CC,CX bond,bond interactions parallel to the increase in the electronegativity of X. For example, Li bonded with two other σ-repellers (CH$_3$ groups) to carbon destabilizes (enhanced interaction of C,C concentrations lumps) while F stabilizes 2-propane.

VI. Conclusion

The principle of avoidance of geminal and vicinal charge concentration provides a guideline to predict structural and energetic features of substituted cyclopropanes and molecules topologically related to cyclopropanes. Although many of the descriptive terms used in this paper may remind one of an electrostatic description of interactions between atoms, it has to be stressed that *the electron-density model developed is not an electrostatic model* since it is based on the behavior of *both the potential energy density V(r) and the kinetic energy density G(r)*

as covered by the Laplacian of $\rho(r)$ (see eq 2).

Also, it is important to note that the electron density model of 3MRs does not simply rephrase the facets of the Walsh MO model. The difference between the two models becomes apparent when considering the F substituent, once as a "π-donor" and once as a "π-repeller". While in the MO picture it is reasonable to speak of a charge transfer from the lone-pair pπ orbitals of F to the Walsh MOs of the 3MR, such a charge transfer is not obvious from the density and concentration distribution calculated for either **2** or **10**. The F atom is strongly electronegative, pulling electron density toward its nucleus from all directions and concentrating it in the way revealed by $-\nabla^2\rho(r)$. There is no indication of a "recycling process" of density in a σ-acceptor/π-donor fashion. F causes only a redistribution of charge at the neighboring atom. Observations like this have led us to refrain from classifying substituents in "donors" and "acceptors" as is usually done in MO theory.

One has also to realize that $\rho(r)$ and all its properties lead to a "static" description of the molecule, i.e., they provide a priori no answer to questions such as "what happened when the atoms came together and formed the molecule?". However, the two-step analysis of $\rho(r)$ and $\nabla^2\rho(r)$ presented above offers some insight into this problem. For example, the investigation of compounds **1–20** suggests a relatively simple pattern of atom,atom interactions, which can be used for predictive purposes. The observation that geminal and vicinal charge concentrations try to avoid each other suffices to rationalize substituent,ring interactions of cyclopropanes also in those cases where the Walsh model is difficult to apply.

(16) Cremer, D.; Kraka, E., to be published.
(17) HF/6-31G* geometries have been taken from the following: DeFrees, D.; Levi, B. A.; Pollack, S. K.; Hehre, W. J.; Binkley, J. S.; Pople, J. A. *J. Am. Chem. Soc.* **1979,** *101,* 4085–4089.

Picosecond Dynamics of the Paterno–Buchi Reaction

Steven C. Freilich[†] and Kevin S. Peters[*‡]

Contribution from the Department of Chemistry, Harvard University, Cambridge, Massachusetts 02138. Received October 30, 1984

Abstract: The photocycloaddition of aromatic ketones and electron-rich olefins is found to proceed through the formation of a 1,4-biradical, and the absorption spectrum of the transient is reported in the reactions of benzophenone and xanthone with 1,4-dioxene. The biradical is found to be unstable, and one mode of decay of the species is heterolysis to a contact ion pair. The mechanism for the cycloaddition is discussed in terms of direct formation of the biradical without the intermediacy of an exciplex or charge-transfer species.

The photocycloaddition reaction of an olefin to a ketone, the Paterno–Buchi reaction,[1,2] has been the subject to numerous investigations owing to the importance of its synthetic utility. The mechanistic studies of Arnold[3] on triplet-state reaction of the ketone suggested that an intermediate between the excited state and product must intervene along the reaction coordinate. This was principally based upon the demonstration that the photoreaction of benzophenone with *cis-* or *trans-*2-butene yields es-

sentially the same mixture of the *cis-* and *trans-*oxetane (1:9) regardless of the stereochemistry of the starting olefin. These results suggested the intermediacy of a 1,4-biradical species that would allow for free rotation about the terminal bond.

Despite the success of the 1,4-biradical hypothesis, there is some evidence which intimates a more complicated picture of the reaction profile. The exceptions to the most stable biradical rule and the apparent anomolous deuterium isotope effect led Caldwell[4]

†Current address: Central Research and Development, E. I. du Pont de Nemours and Company, Experimental Station, Wilmington, Delaware 19898.
‡Current address: Department of Chemistry, University of Colorado, Boulder, Colorado 80309.

(1) Paterno, E.; Chiefi, G. *Gazz. Chim. Ital.* **1909,** *39,* 431.
(2) Buchi, G.; Inman, C. G.; Lipinsky, E. S. *J. Am. Chem. Soc.* **1954,** *76,* 4327.
(3) Arnold, D. R. *Adv. Photochem.* **1968,** *6,* 301.